

Immersed-boundary simulations of turbulent flow past a slowly varying river bottom

P. Luchini



DIIN, Università di Salerno, 84084 Fisciano, Italy

VORTICAL STRUCTURES AND WALL TURBULENCE

Paolo Orlandi: A vortical and turbulent life

19–20 September 2014

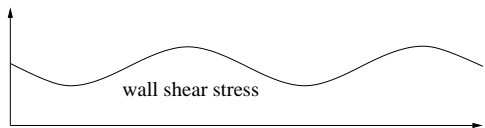
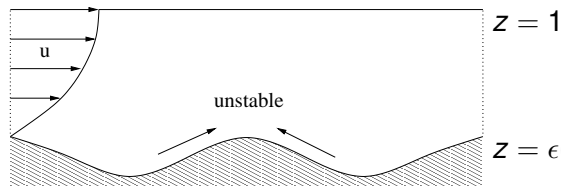
Centro Congressi Villa Mondragone – Monteporzio Catone

A classical problem: formation of ripples and dunes

(e.g. Bagnold 1941; Charru, Andreotti & Claudin 2012).

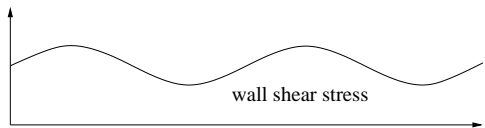
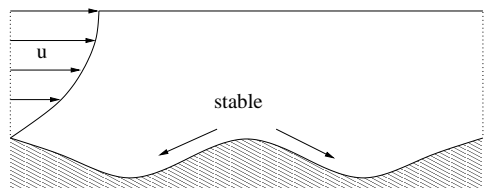
Adapted from Charru *et al.*, *Annu. Rev. Fluid Mech.* 2012:

The steady or oscillatory motion of a liquid above a granular bed leads to the formation of ripples. The sand ripples one observes on a beach at low tide are an example: these ripples were formed by the oscillations induced by the surface waves when the beach was covered with shallow water. The mechanism of their formation, related to fluid inertia, sits in the relative phase of bottom shear stress oscillations with respect to oscillations of the bottom itself, with positive phase advance of the shear stress dragging the particles toward crests during each half-period. The net particle flux toward crests can also be understood as the result of the mean steady drift flow (steady streaming). Similar structures are also observed on the continental shelf at water depths of 200–300 m, with a wavelength of the order of 1 m.



$$\frac{\delta\tau}{\epsilon} = \tau_C^{(1)} \cos kx + \tau_S^{(1)} \sin kx$$

$\tau_S^{(1)} < 0$: unstable.



$\tau_S^{(1)} > 0$: stable.

Laminar flow

Linearized solution = steady Orr-Sommerfeld equation

$$(\psi_{zz} - k^2\psi)U - \psi U_{zz} = -\frac{1}{ikRe}(\psi_{zzzz} - 2k^2\psi_{zz} + k^4\psi).$$

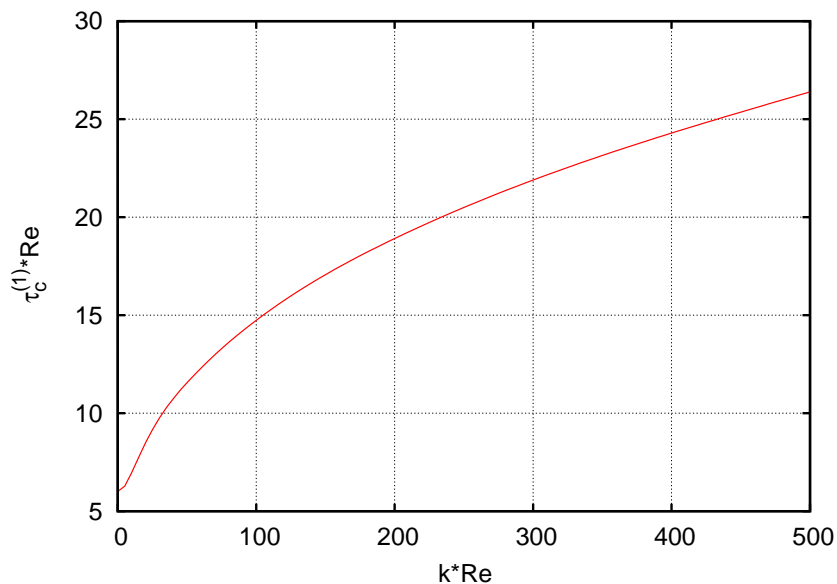
$$U = 3(1 - z/2)z.$$

$$\psi(0) = 0; \quad \psi_z(0) = -3; \quad \psi(1) = 0; \quad \psi_{zz}(1) = 0.$$

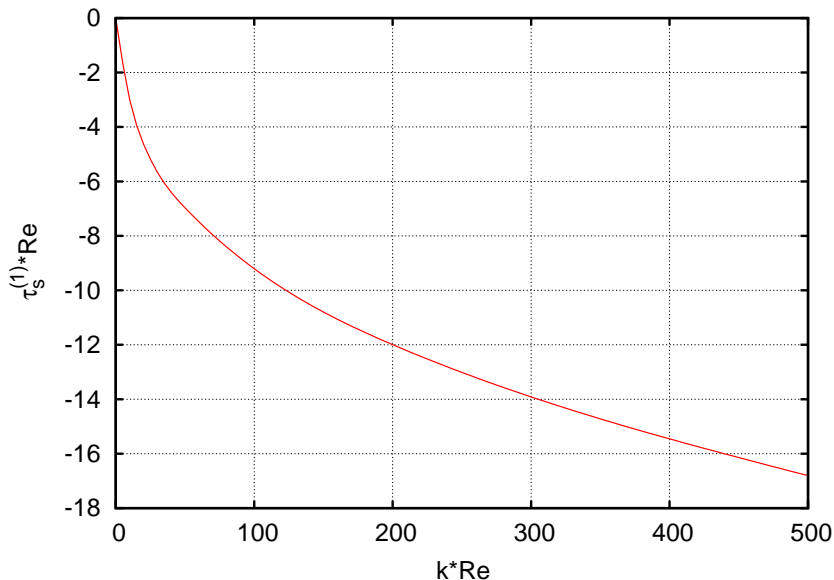
$$\tau_c^{(1)} + i\tau_s^{(1)} = \psi_{zz}(0) - 3$$

Two parameters: k^2 and kRe .
 k^2 may often be neglected.

Laminar flow: in-phase component of wall shear stress

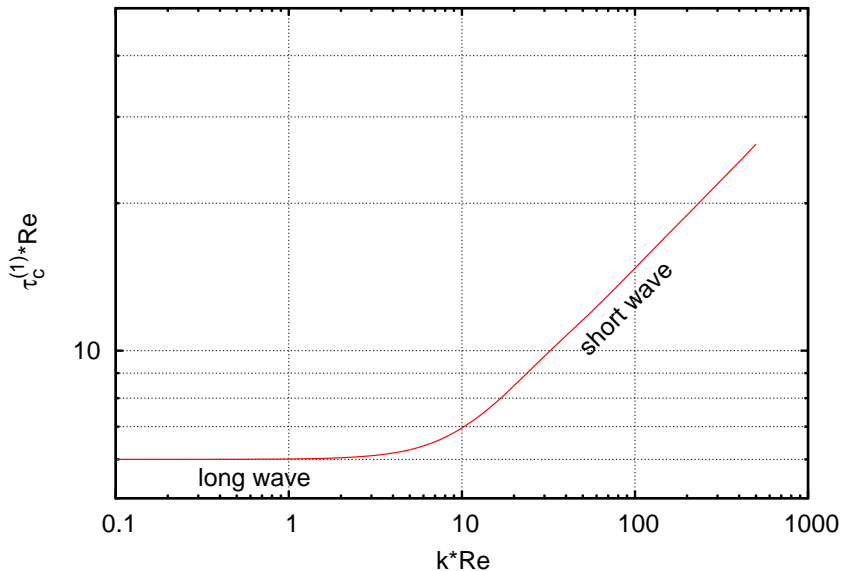


Laminar flow: quadrature component

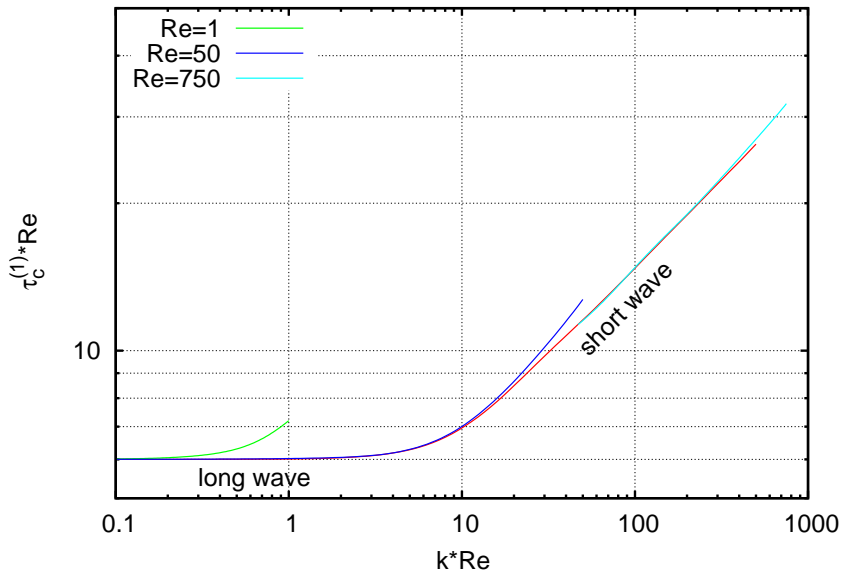


Note: erodible bottom is unstable at all wavenumbers.

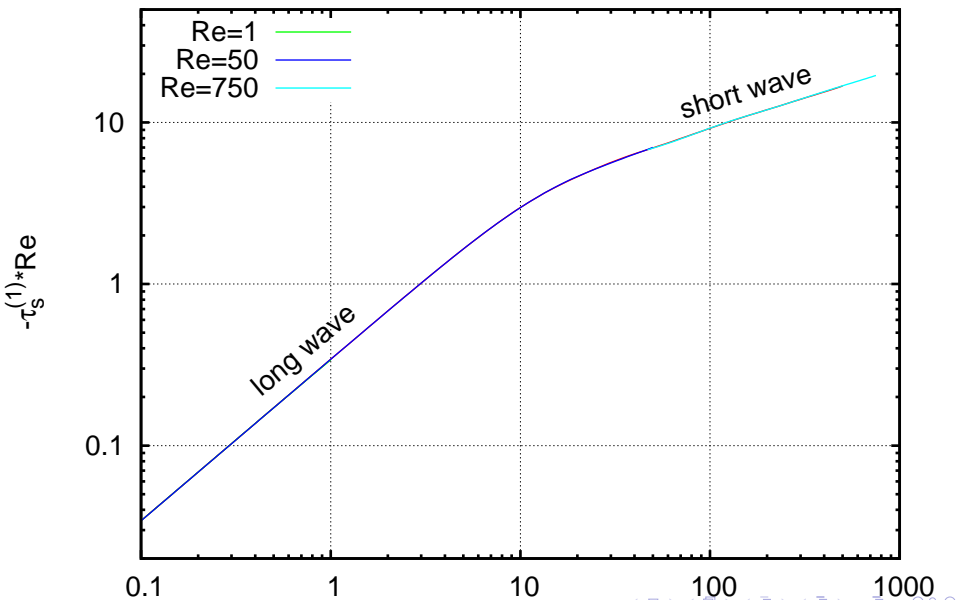
In-phase component in logarithmic scale



The relevance of k^2



Quadrature component in logarithmic scale



Limiting cases

Short-wave (boundary-layer) approximation

- Benjamin, T. B. 1959 (laminar)
- Jackson, P. S. & Hunt, J. C. R. 1975 (turbulent)
- Belcher, S. E. & Hunt, J. C. R. 1998 (turbulent)

Long-wave (shallow-water) approximation

- Benjamin, T. B. 1957 (laminar)
- Yih, C. S. 1963 (laminar)
- Shkadov, Blondeaux, Colombini, many more...
- Luchini, P. & Charru, F. 2010 (laminar & turbulent)

All use an eddy viscosity model to represent turbulence.

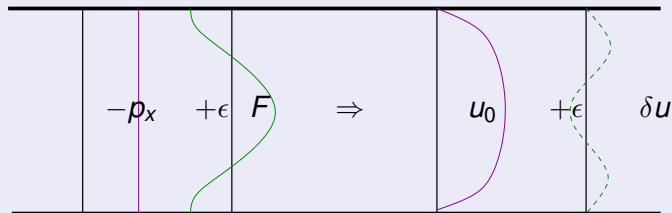
All predict negative quadrature component (**unstable** erodible bottom).

Experiments by Hanratty *et al.* (~ 1980, not really long wave) confirm negative quadrature component.

But...

A key step in the procedure by Luchini & Charru (2010) was the reduction of the effect of the slowly variable depth to an equivalent volume force.

The response of channel flow to a volume force

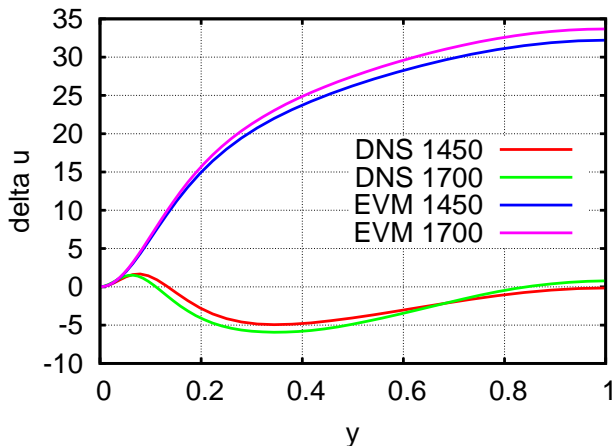


Pressure gradient + Volume force \Rightarrow Velocity profile + ?

was analysed through direct numerical simulation.

Simple enough problem to afford a **head-to-head comparison** between eddy viscosity and DNS.

Luchini, P. & Russo, S., APS DFD 2011: Comparison



Re	$\delta Q(\text{EVM})$	$\delta Q(\text{DNS})$
1450	23.65	-4.43
1700	24.74	-5.12

Luchini, P. & Russo, S., APS DFD 2011: Conclusions

- 1 The linear response of a channel flow to a small volume force provides a valuable test bed for the comparison of DNS and turbulence models.
- 2 The DNS results are essentially different, and even of opposite sign, than the predictions of a common eddy-viscosity model. Provably, no (positive) eddy viscosity can match the DNS.
- 3 Turbulence-convection models are not going to change this conclusion, since in a parallel flow convection has no role.
- 4 For applications such as flow along a variable bottom, the **quadrature component** of wall shear stress turns out to be **positive**: the **erodible bottom** is **stable** against long waves.

Immersed-boundary simulation of flow past a wavy bottom

- Second-order finite differences in all directions. Stretched coordinate along wall-normal z coordinate only. Fully parallel. Explicit time advancement for all but the pressure-correction equation.

Immersed-boundary simulation of flow past a wavy bottom

- Second-order finite differences in all directions. Stretched coordinate along wall-normal z coordinate only. Fully parallel. Explicit time advancement for all but the pressure-correction equation.
- Immersed-boundary implementation uses internal (to the fluid) points only; is continuous with respect to boundary crossing and stable in iteration at all distances from the boundary. It was tested in a previous Stokes-flow application (Luchini, JFM 2013).

Immersed-boundary simulation of flow past a wavy bottom

- Second-order finite differences in all directions. Stretched coordinate along wall-normal z coordinate only. Fully parallel. Explicit time advancement for all but the pressure-correction equation.
- Immersed-boundary implementation uses internal (to the fluid) points only; is continuous with respect to boundary crossing and stable in iteration at all distances from the boundary. It was tested in a previous Stokes-flow application (Luchini, JFM 2013).
- The most delicate part is evaluating the wall shear stress. Common solution of summing virtual forces is not sufficient: the contribution of pressure gradient over fractional cell boundaries is of the same order as the effect under investigation.

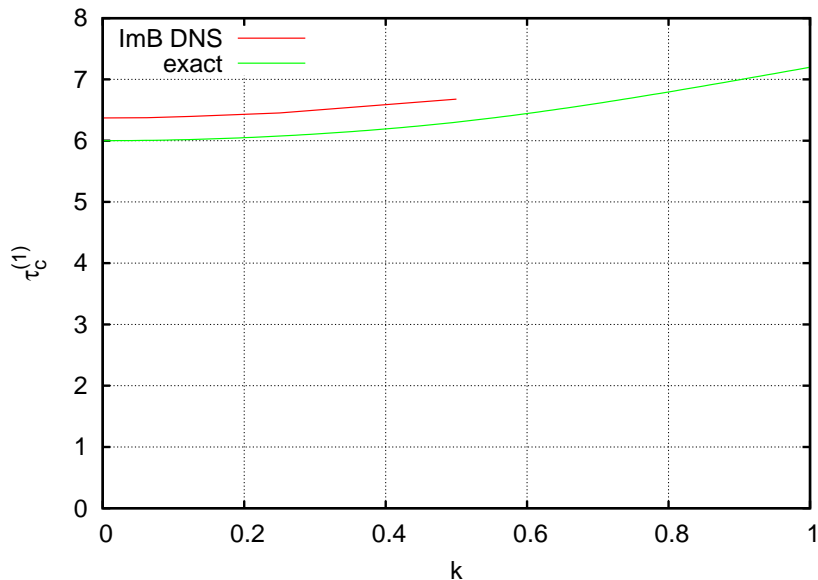
Immersed-boundary simulation of flow past a wavy bottom

- Second-order finite differences in all directions. Stretched coordinate along wall-normal z coordinate only. Fully parallel. Explicit time advancement for all but the pressure-correction equation.
- Immersed-boundary implementation uses internal (to the fluid) points only; is continuous with respect to boundary crossing and stable in iteration at all distances from the boundary. It was tested in a previous Stokes-flow application (Luchini, JFM 2013).
- The most delicate part is evaluating the wall shear stress. Common solution of summing virtual forces is not sufficient: the contribution of pressure gradient over fractional cell boundaries is of the same order as the effect under investigation.
- The amplitude ϵ of the wall oscillation has to strike a compromise between linearity and statistical fluctuation error of time averaging.

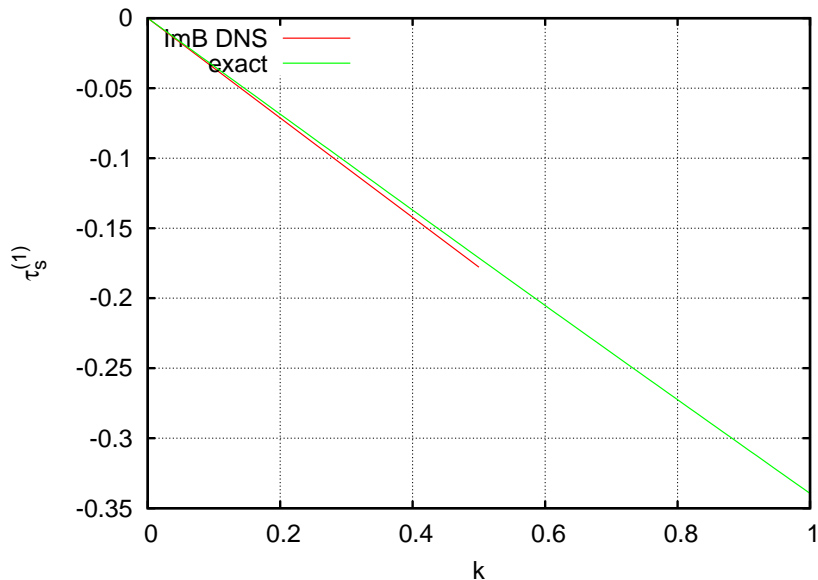
Immersed-boundary simulation of flow past a wavy bottom

- Second-order finite differences in all directions. Stretched coordinate along wall-normal z coordinate only. Fully parallel. Explicit time advancement for all but the pressure-correction equation.
- Immersed-boundary implementation uses internal (to the fluid) points only; is continuous with respect to boundary crossing and stable in iteration at all distances from the boundary. It was tested in a previous Stokes-flow application (Luchini, JFM 2013).
- The most delicate part is evaluating the wall shear stress. Common solution of summing virtual forces is not sufficient: the contribution of pressure gradient over fractional cell boundaries is of the same order as the effect under investigation.
- The amplitude ϵ of the wall oscillation has to strike a compromise between linearity and statistical fluctuation error of time averaging.
- An ad hoc algorithm was developed to estimate the expected error of the time average.

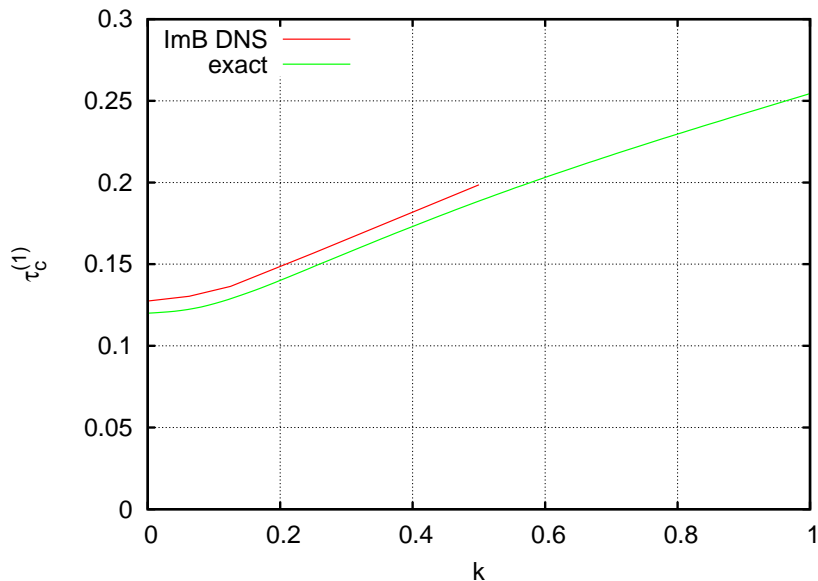
Laminar test: $Re = 1$



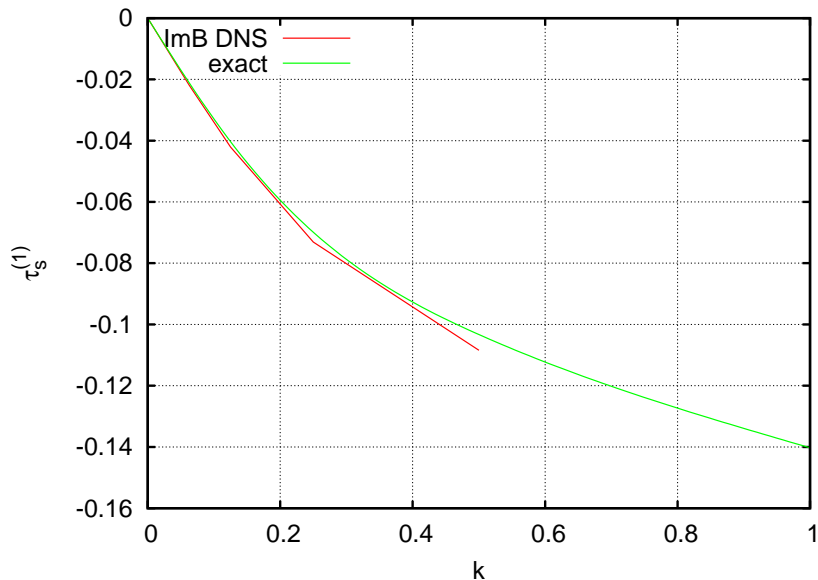
Laminar test: $Re = 1$



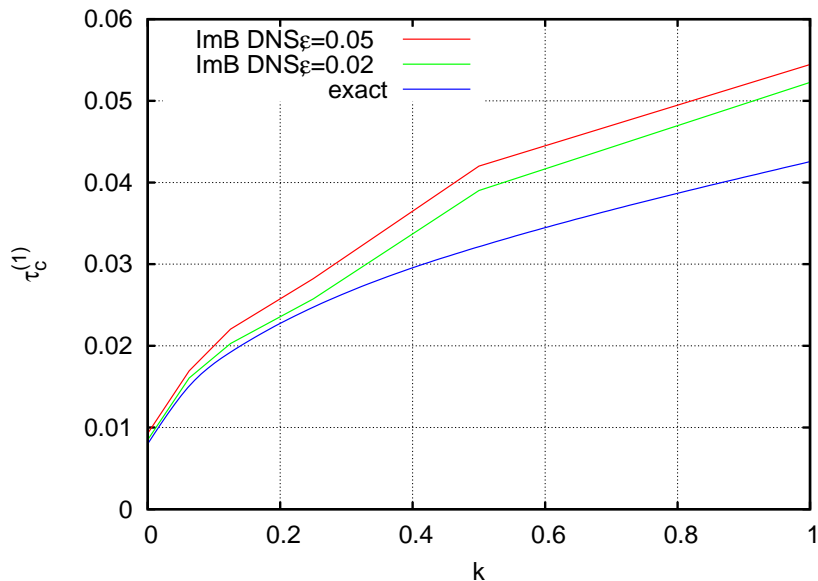
Laminar test: $Re = 50$



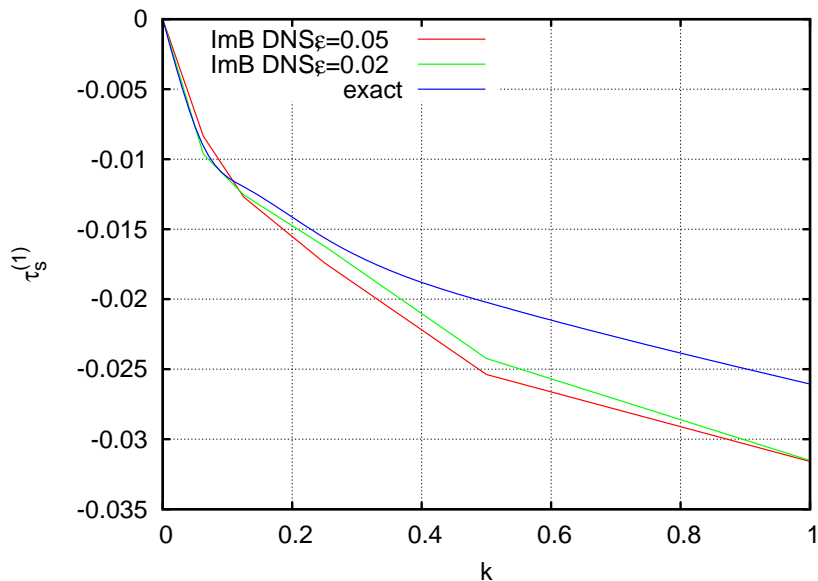
Laminar test: $Re = 50$



Laminar test: $Re = 750$

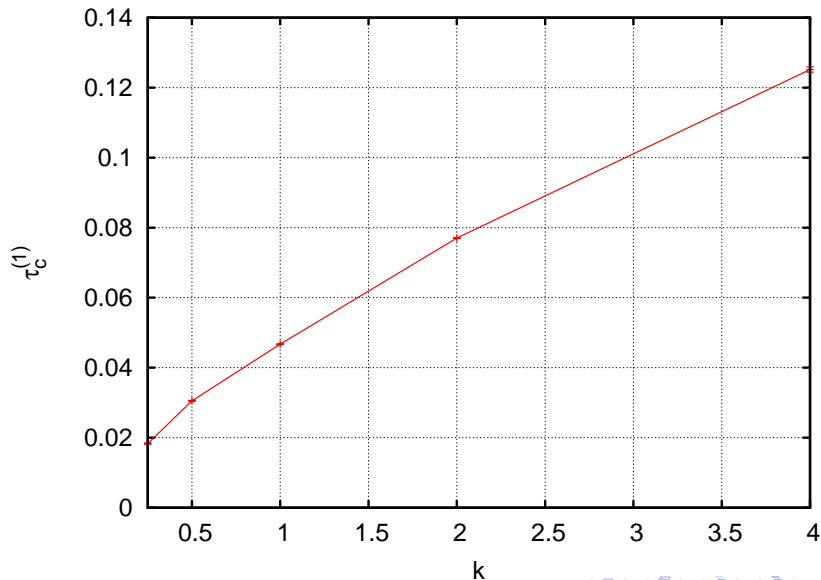


Laminar test: $Re = 750$



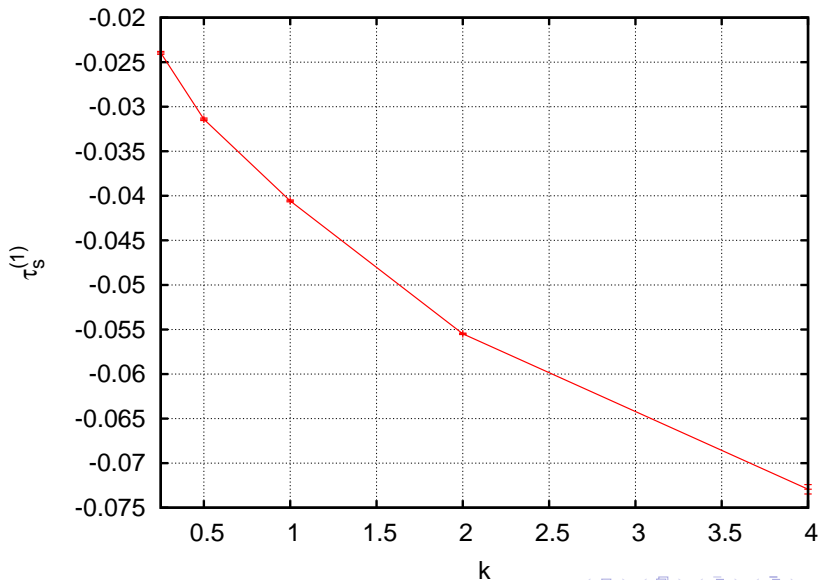
Turbulent channel: in-phase shear stress

$Re = 1450$ ($Re_\tau = 100$); computational box up to 8π .



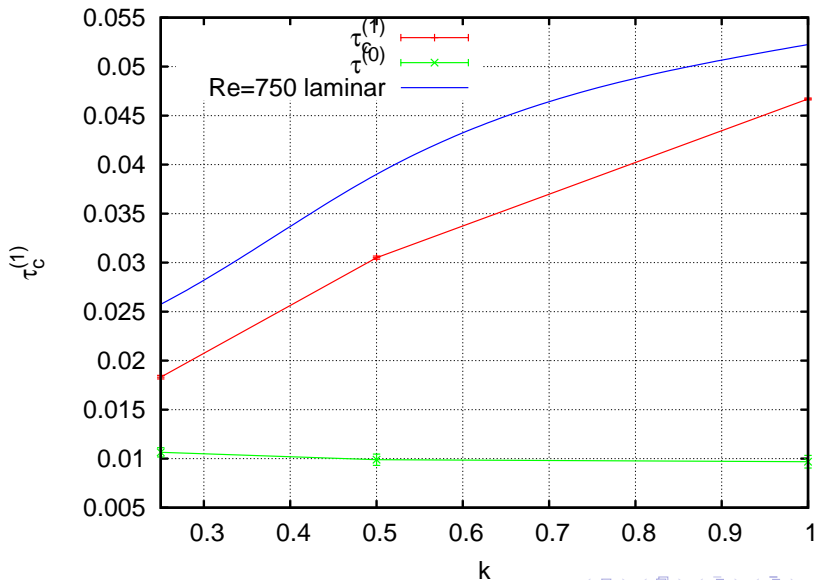
Turbulent channel: quadrature shear stress

$Re = 1450$ ($Re_\tau = 100$); computational box up to 8π .



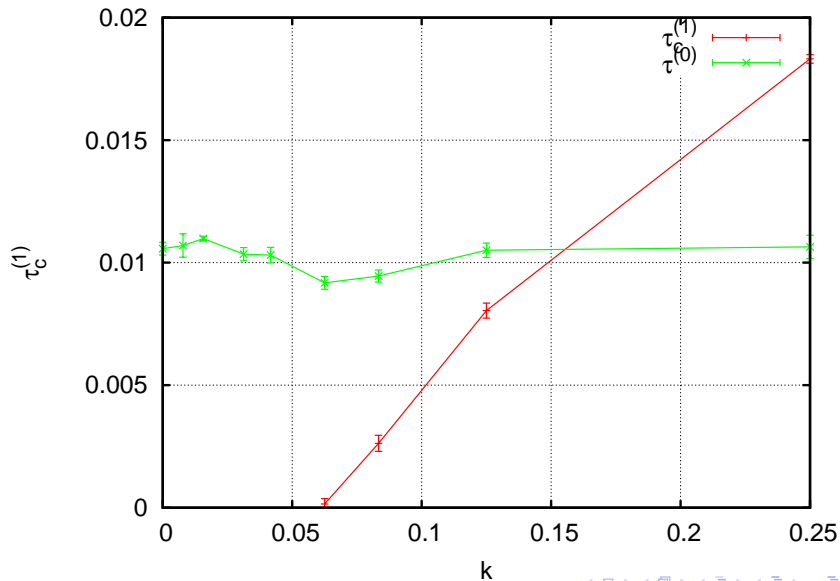
Turbulent channel: in-phase shear stress

$Re = 1450$ ($Re_\tau = 100$); computational box up to 8π .



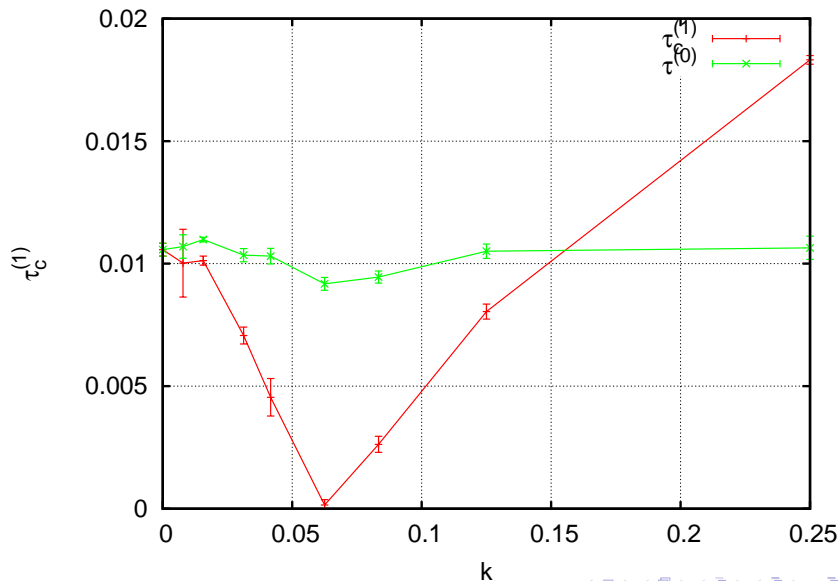
Turbulent channel: in-phase shear stress

$Re = 1450$ ($Re_\tau = 100$); computational box up to 32π .



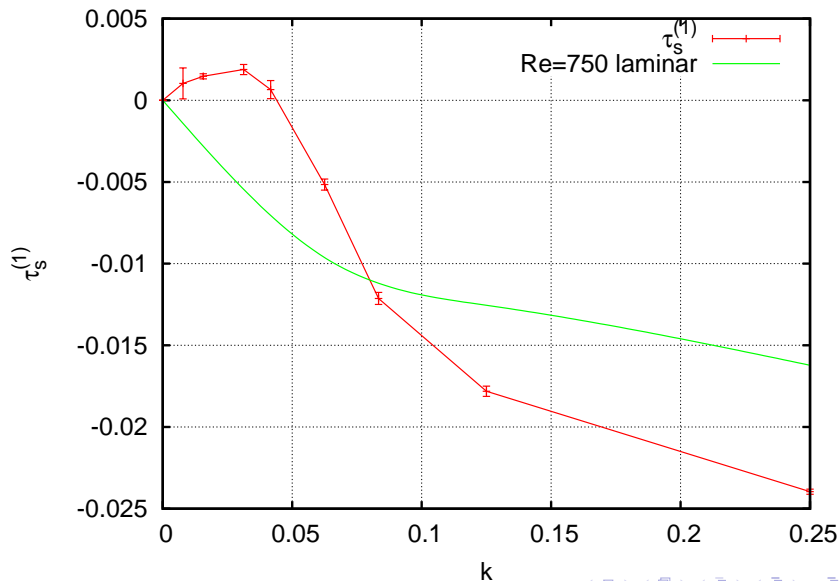
Turbulent channel: in-phase shear stress

$Re = 1450$ ($Re_\tau = 100$); computational box up to 32π and beyond...



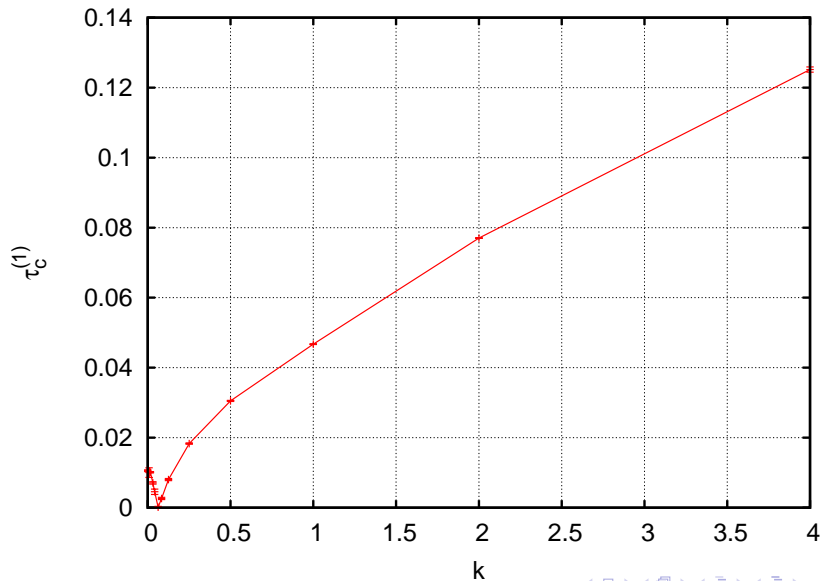
Turbulent channel: quadrature shear stress

$Re = 1450$ ($Re_\tau = 100$); computational box up to 256π .



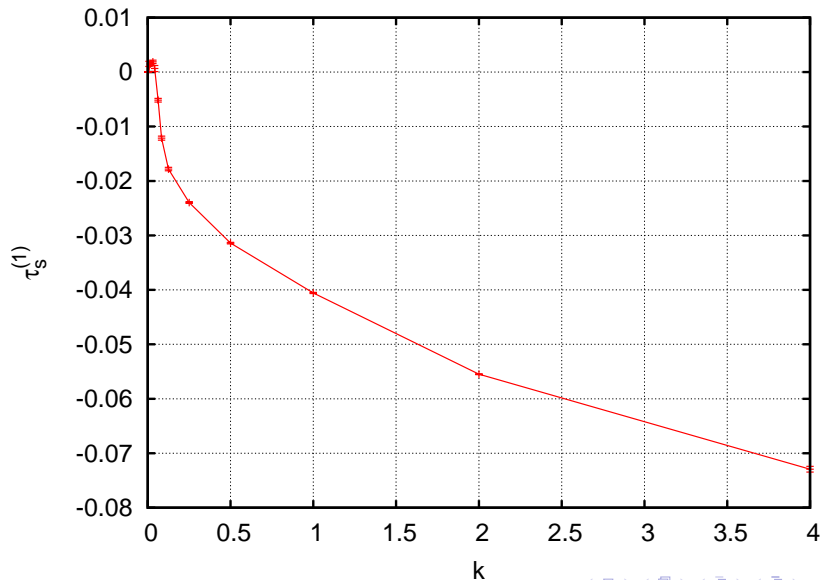
Turbulent channel: in-phase shear stress

$Re = 1450$ ($Re_\tau = 100$).



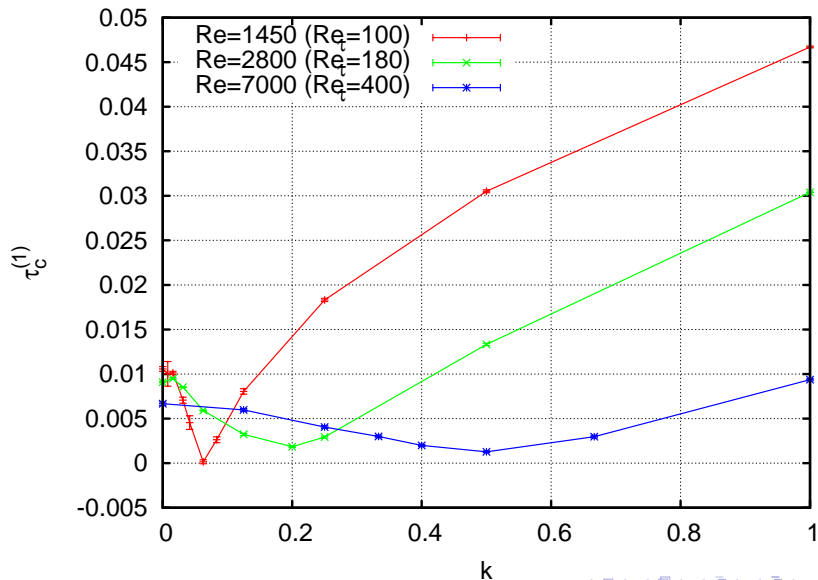
Turbulent channel: quadrature shear stress

$Re = 1450$ ($Re_\tau = 100$).



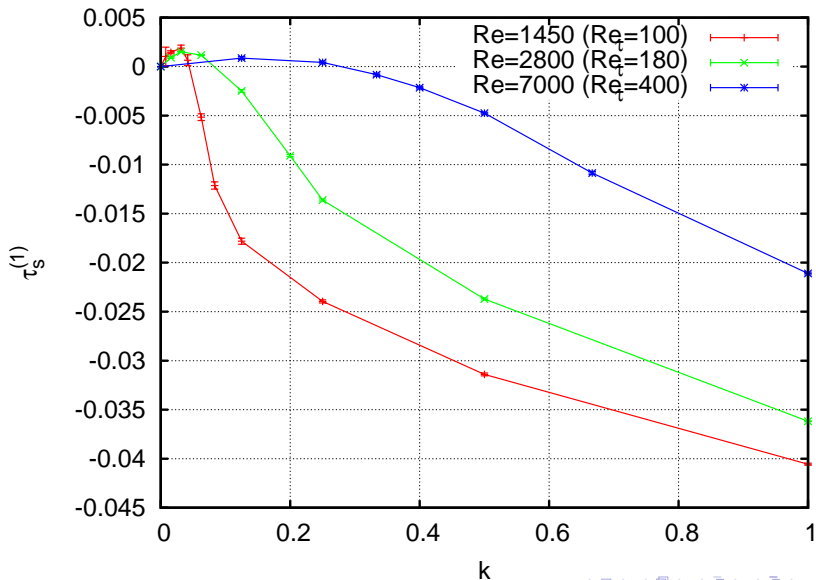
Turbulent channel: in-phase shear stress

Effect of Reynolds number

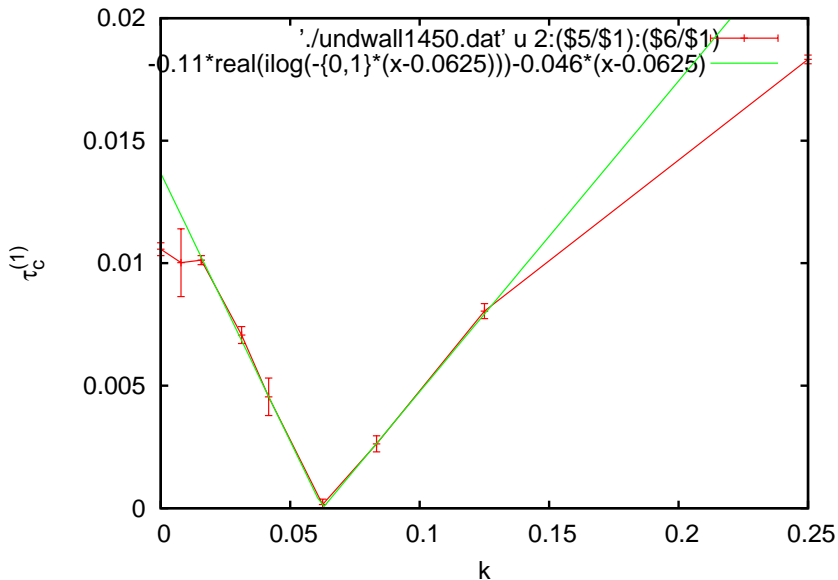


Turbulent channel: quadrature shear stress

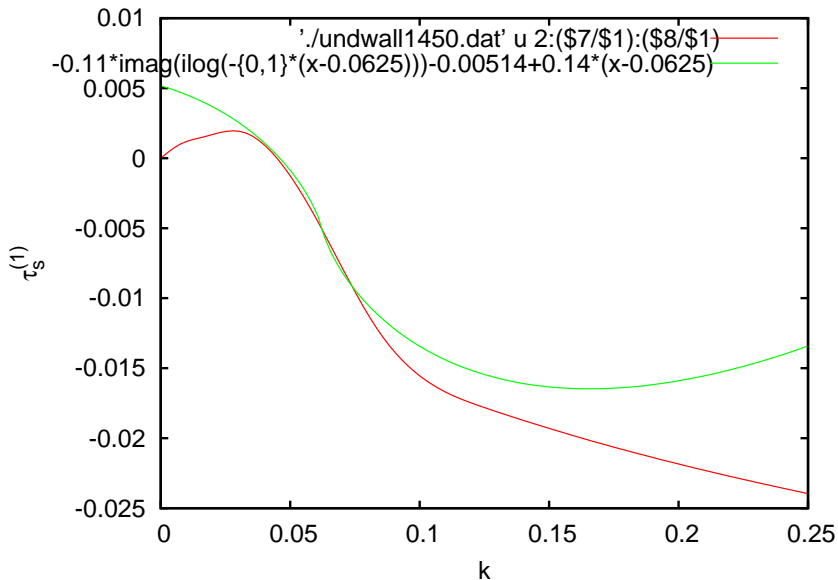
Effect of Reynolds number



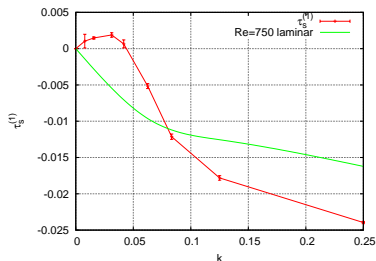
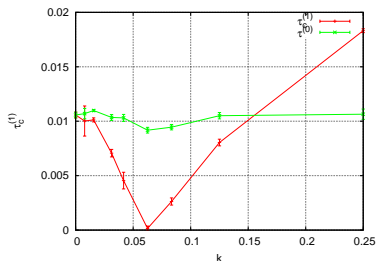
Is it really a singularity? tentative fit.



Is it really a singularity? tentative fit.



Conclusions



- Turbulent flow past a wavy river bottom exhibits interesting behaviour at unexpectedly large wavelength. This behaviour is only visible with periodic computational boxes **longer than 32π** .
- In striking contrast to laminar flow (and to all turbulence models), the long-wave quadrature shear stress is **positive**.
- The findings of Luchini & Russo 2011 are thus confirmed. They are not in contrast with experiment because no experiment has been conducted at such large wavelength.
- The mean linear response of turbulent flow exhibits what may look like a **singularity** at transition Reynolds number.